Recent results from the cosmic ray program of the NA61/SHINE experiment

Raul R. Prado[1,2,3,*] for the NA61/SHINE Collaboration[**]

[1]Deutsches Elektronen-Synchrotron (DESY), Platanenallee 6, D-15738 Zeuthen, Germany
[2]IKP, Karlsruhe Institute of Technology (KIT), Postfach 3640, D-76021 Karlsruhe, Germany
[3]Instituto de Física de São Carlos (IFSC/USP), Av. Trabalhador São-carlense 400, 13566-590, São Carlos, Brazil

Abstract. NA61/SHINE is a fixed target experiment designed to study hadron-proton, hadron-nucleus and nucleus-nucleus interactions at the CERN Super-Proton-Synchrotron. In this paper we summarize the results from pion-carbon collisions recorded at beam momenta of 158 and 350 GeV/c. Hadron production measurements in these types of interactions is of fundamental importance for the understanding of the muon production in extensive air showers. In particular, production of (anti)baryons and ρ^0 are mechanisms responsible for increasing the number of muons which reach the ground. The underestimation of the (anti)baryons or ρ^0 production rates in current hadronic interaction models could be one of the sources of the excess of muons observed by cosmic ray experiments. The results on the production spectra of $\pi^\pm$, K$^\pm$, p, p̄, Λ, $\bar{\Lambda}$, K$_S^0$, ρ^0, ω and K^{*0} are presented, as well as their comparison to predictions of hadronic interaction models currently used in air shower simulations.

1 Introduction

Measurements of ultrahigh energy cosmic rays are only possible through the detection of secondary particles produced in extensive air showers (EAS). The inference of some of the properties of the primary cosmic ray particles like their nuclear mass, relies on the comparison of measured EAS observables to predictions from simulations [1]. These simulations are performed by Monte Carlo codes that make use of hadronic interaction models to describe the nucleus-air and hadron-air collisions along the shower development [2]. Although simulations using recent hadronic models can provide a good overall description of EAS, it has been observed by cosmic ray experiments that the hadronic models fail on describing the muon production in EAS. Measurements by HiRes-MIA [3], Pierre Auger Observatory [4–7], Telescope Array [8], KASCADE-Grande [9], IceTop/IceCube [10] and Sugar [11] show that there is an inconsistency between data and simulations for observables related to the muonic component of air showers. In particular, the number of muons (N_μ) obtained from simulations is observed to be significantly smaller than the measured ones, which is known as the "muon deficit problem".

The majority of muons in EAS are produced by the decay of charged mesons, which in turn, are produced in meson-air and nucleon-air interactions. Depending on the primary energy and detection distance, the relevant meson-air and nucleon-air interaction energies are between 10 and 1000 GeV [12, 13]. Therefore, measurements of particle production in this energy range are of great value for understanding muon production in EAS and consequently for improving its modeling. Of particular interest are the production spectra of (anti-)baryons and ρ^0 in meson-air and nucleon-air. It is well known [14, 15] that the production of (anti-)baryons and ρ^0 mesons in hadronic interactions is important to predict the muon content of air showers. Therefore the production cross sections of these particles needs to be known accurately for a precise modeling of air showers

NA61/SHINE experiment [16] (see Sec. 2) has provided a number of particle production and cross section measurements which are relevant for the modeling of hadronic interaction in EAS (e.g. Refs [17, 18]). In this paper, however, the focus will be on the results of the 2009 run with a negatively charged pion beam colliding against a thin carbon target (π^-+C data) at 158 and 350 GeV/c. Since π-air is the most abundant hadronic interaction occurring in an EAS, our π^-+C data is of high relevance for the tuning of hadronic interaction models dedicated to EAS simulations. The results are presented in three parts: the spectra of charged hadrons ($\pi^\pm$, K$^\pm$, p and p̄) are presented in Sec. 3, the spectra of V^0 mesons (Λ, $\bar{\Lambda}$ and K$_S^0$) in Sec. 4 and the spectra of resonance mesons (ρ^0, K^{*0} and ω) in Sec. 5.

2 The NA61/SHINE experiment

NA61/SHINE (SHINE = SPS Heavy Ion and Neutrino Experiment) is a fixed target experiment at the CERN SPS designed to study hadron production in nucleus-nucleus and hadron-nucleus collisions. Its physics goals comprise a) the strong interaction program, which investigates the properties of the onset of deconfinement and search for the critical point of strongly interacting matter, b) the neutrino program, to precisely measure the hadron production important to calculate the neutrino and antineutrino fluxes in the T2K neutrino experiment [19], and c) the cosmic ray program, focused on the measurements of the hadron and
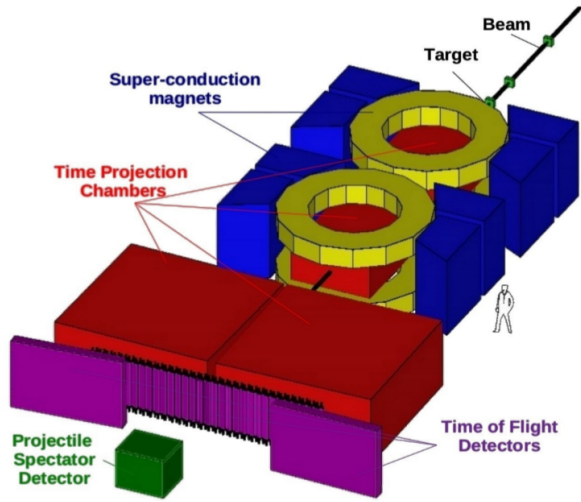
*e-mail: raul.prado@desy.de
**Full author list: http://shine.web.cern.ch/content/author-list

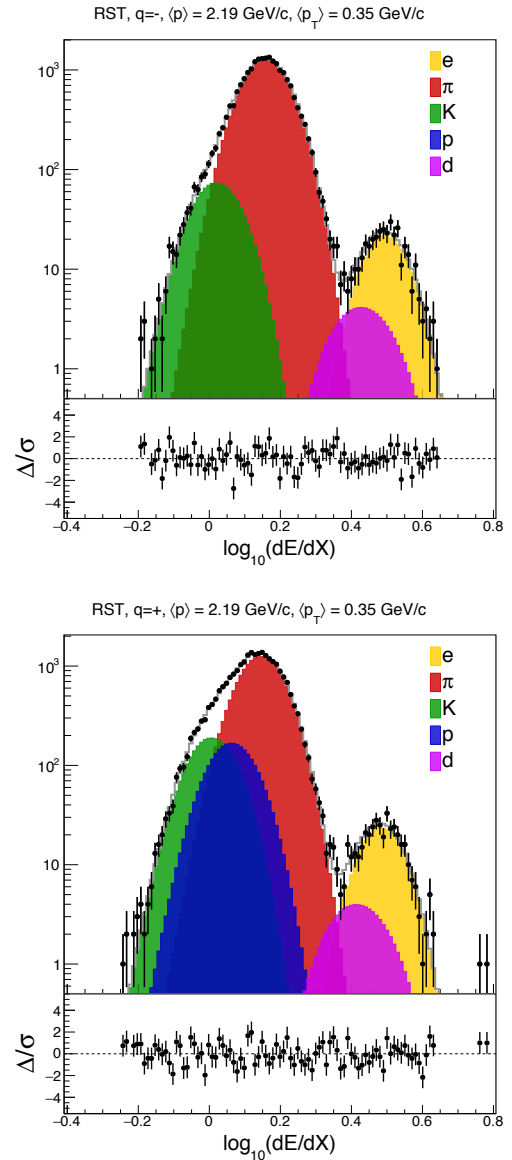Figure 1: Schematic layout of the NA61/SHINE experiment [16].

Figure 2: Example of the dE/dx distributions for one phase space bin ($\langle p \rangle$ = 2.19GeV/c and $\langle p_{\mathrm{T}} \rangle$ = 0.35GeV/c) of the 158 GeV/c data set. The black markers show the measured distributions and the colored distributions show the result of the dE/dx fit. Negatively charged particles are shown on the top and positively ones on the bottom.

meson production which are most relevant for the modeling of extensive air showers. The full description of the NA61/SHINE experiment and its science program can be found in Ref. [16]

The NA61/SHINE detector measures charged particles produced by the collision of the beam particles with the target through a set of five Time Projection Chambers (TPC). Since two of the TPCs are placed in the magnetic field produced by superconducting dipole magnets, the charge and the momenta of the particles can be measured and the achieved resolution on p is of the order of $\sigma(p)/p^2 = 10^{-4}$ (GeV/c)$^{-1}$. Additionally, the energy loss per unit of length (dE/dx) in the TPCs is used in this work for particle identification. The experimental layout of the NA61/SHINE detector is shown in Fig. 1.

A beam detector system composed of scintillation and Cherenkov counters is placed upstream of the detector to identify and measure the beam particles. The position of the beam is measured by a set of three beam position detectors, which are also placed upstream of the target.

3 Production of $\pi^{\pm}$, K$^{\pm}$, p and p̄

Charged particles are identified in NA61/SHINE by the track-by-track measurement of the deposited energy, dE/dx, performed by the TPCs. After splitting the data into bins of total and transverse momentum (p and p_{T}), a dE/dx model is fitted to the measured dE/dx distributions by accounting for contributions of 5 particle types (e, π, K, p and deuterons). From the results of the fit, the particle yields of $\pi^{\pm}$, K$^{\pm}$ and p(p̄) are determined. Examples of measured dE/dx distributions and of the results of the dE/dx fit are shown in Fig. 2. After performing the particle identification through the dE/dx fit, the detector effects (e.g. acceptance, efficiency) are corrected by using a set of Monte Carlo simulations and the spectra are derived. A more detailed description of the analysis procedure can be found in Ref. [20].

The single-differential spectra as a function of p (integrated over p_{T}) for $\pi^{\pm}$, K$^{\pm}$ and p(p̄) are shown in Figs. 5

and 6, where the measurements are compared to the predictions of Epos 1.99 [14], Sibyll 2.1 [21], Sibyll 2.3 [22], QGSJet II-04 [23] and Epos LHC [24]. The double-differential spectra as a function of p and p_{T} can be found in Ref. [25] for the $\pi^{\pm}$ spectra and in Ref. [20] for the K$^{\pm}$ and p(p̄) spectra.

4 Production of Λ, $\bar{\Lambda}$ and K$_{\mathrm{S}}^{0}$

Since $\Lambda(\bar{\Lambda})$ and K$_{\mathrm{S}}^{0}$ are neutral weakly decaying particles, they can be measured by NA61/SHINE through the detection of the charged particles which are produced in their decays. The invariant mass (m_{inv}) spectra for a given decay channel can then be used to extract their signal. The decay channels used here are $\Lambda \rightarrow p + \pi^{-}$, $\bar{\Lambda} \rightarrow \bar{p} + \pi^{+}$,
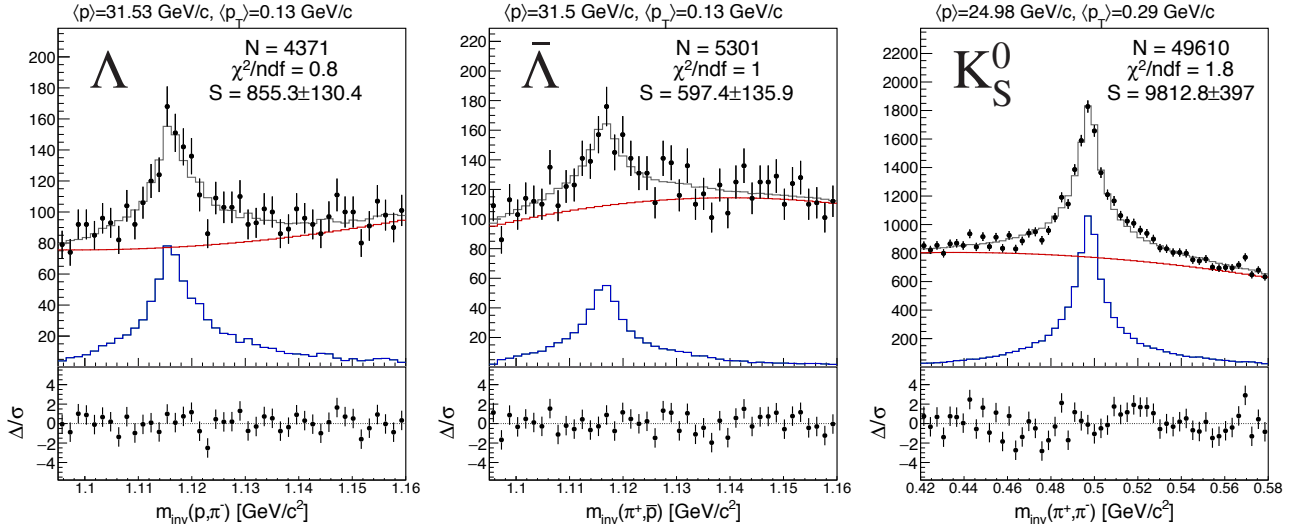
Figure 3: Example of the m_{inv} distributions for one phase space bin ($\langle p \rangle$ and $\langle p_T \rangle$ are indicated on the top of each plot) of the 158 GeV/c data set. The black markers show the measured distributions and the colored lines show the result of the signal extraction fit, where the signal is shown in blue and the background in red.

$K_S^0 \rightarrow \pi^+ + \pi^-$. To extract the signal, the m_{inv} distributions were fitted by considering a signal contribution, modeled by using Monte Carlo templates, and the background, modeled by a 2nd-degree polynomial function. Examples of the fitted m_{inv} distributions are shown in Fig. 3.

This analysis was performed in 2-dimensional phase space bins of p and p_T. For each phase space bin, the detector effects were corrected by using Monte Carlo simulations. The full double-differential spectra as a function of p and p_T for $\Lambda(\bar{\Lambda})$ and K_S^0 at 158 and 350 GeV/c can be found in Ref. [26]. In Figs. 7 and 8 we show the measured single-differential spectra as function of p (integrated over p_T) together with predictions of the hadronic models.
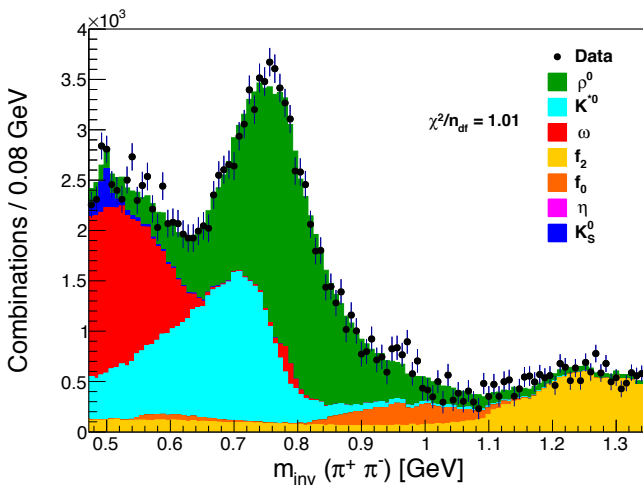
5 Production of ρ^0, K^{*0} and ω

Figure 4: Example of the $m_{inv}(\pi^+\pi^-)$ distribution for one x_F bin ($0.3 < x_F < 0.4$) of the 158 GeV/c data set. The black markers show the measured distributions and the colored distributions show the results of the template fit.

By using the NA61/SHINE apparatus, the yields of ρ^0, K^{*0} and ω can be measured through the $\pi^+\pi^-$ invariant mass ($m_{inv}(\pi^+\pi^-)$) spectra. The signal extraction is performed by fitting Monte Carlo templates to the measured $m_{inv}(\pi^+\pi^-)$ distribution. The Monte Carlo events were generated using Epos 1.99 as hadronic interaction model and they were passed through the full NA61/SHINE detector simulation and reconstruction chain. The estimation of the combinatorial background were done by two methods: the charge mixing method, in which the $\pi^+\pi^+$ and $\pi^-\pi^-$ are treated as the background, and the Monte Carlo method, in which the background mass distribution is obtained directly from simulations. One example of the $m_{inv}(\pi^+\pi^-)$ distributions with the results of the template fit is shown in Fig. 4. After the signal extraction, the particle yields were corrected by the detector effects and the production spectra were derived. The full description of the analysis procedure and the results can be found in Ref. [27].

We show in Fig. 9 the obtained ρ^0, K^{*0} and ω spectra together with predictions from simulations with the hadronic models. The ρ^0 spectra are shown for both beam energies, 158 and 350 GeV/c, and the ω and K^{*0} spectra are limited to the 158 GeV/c data set because of the large uncertainties obtained at 350 GeV/c.

6 Summary and conclusions

The NA61/SHINE experiment, within its very rich program, has provided a large number of measurements which have been used for testing and tuning of hadronic interaction models used by the cosmic ray community. In this paper, we have summarized the results of the special cosmic ray runs for $\pi^- + C$ interactions.

First, we have shown the identified spectra of charged hadrons obtained by using the dE/dx measurements. Of particular interest here is the production spectra of $p(\bar{p})$, which are relevant to study the (anti)baryon productions in hadron-air interactions and its implications on the muon

production in EAS. From the p̄ spectra shown in Figs. 5 and 6, one can see that the (anti)baryon production is not underestimated in general by the models. In particular, the Epos model shows to describe very well the p̄ production. As a conclusion, the underproduction of (anti)baryons in π-air interactions by the hadronic models is unlikely to be the most relevant source of the lack of muons in simulations.

Secondly, we have shown the results of the V^0 analysis, aiming at the $\Lambda(\bar{\Lambda})$ and K^0_S spectra. Although these measurements are surely relevant for model testing and tuning, our main motivation here is to reduce the systematic uncertainties on the $\pi^\pm$ and p(p̄) spectra due to the feed-down contributions from weak decays. Since a significant fraction of $\pi^\pm$ and p(p̄) detected are produced by the decay of Λ, $\bar{\Lambda}$ and K^0_S, this effect has to be corrected. In the results shown in Sec. 3 (and in Ref.[20]) this correction is done by using Monte Carlo simulations and the model dependence of this procedure is added to the systematic uncertainties. By measuring the spectra of Λ, $\bar{\Lambda}$ and K^0_S, we are able to avoid this model dependence and consequently reduce the systematic uncertainties. Updated $\pi^\pm$ and p(p̄) spectra with improved systematic uncertainties will be presented in the future in another publication.

Finally, we have shown the final results of the meson resonance analysis which have already been published in Ref. [27]. From the ρ^0 production spectra shown in Fig. 9, one can see that none of the hadronic models can describe well the measurements. The small excess of ρ^0 observed with relation to the predictions from simulations can be relevant to explain the muon deficit in simulations.

Acknowledgments

References

[1] K.H. Kampert, M. Unger, Astroparticle Physics **35**, 660 (2012), `1201.0018`

[2] R. Engel, D. Heck, T. Pierog, Annual Review of Nuclear and Particle Science **61**, 467 (2011)

[3] T. Abu-Zayyad et al. (HiRes/MIA Collaboration), Physical Review Letters **84**, 4276 (2000), `astro-ph/9911144`

[4] A. Aab et al. (Pierre Auger Collaboration), Physical Review **D91**, 032003 (2015), `1408.1421`

[5] A. Aab et al. (Pierre Auger Collaboration), Physical Review Letters **117**, 192001 (2016), `1610.08509`

[6] A. Aab et al. (Pierre Auger Collaboration), Physical Review **D90**, 012012 (2014), `1407.5919`

[7] A. Aab et al. (Pierre Auger Collaboration), Physical Review **D96**, 122003 (2017), `1710.07249`

[8] R.U. Abbasi et al. (Telescope Array Collaboration), Phys. Rev. **D98**, 022002 (2018), `1804.03877`

[9] W.D. Apel et al. (KASCADE-Grande Collaboration), Astroparticle Physics **95**, 25 (2017)

[10] H. Dembinski (IceCube Collaboration), EPJ Web of Conferences **145**, 01003 (2017)

[11] J.A. Bellido, R.W. Clay, N.N. Kalmykov, I.S. Karpikov, G.I. Rubtsov, S.V. Troitsky, J. Ulrichs, Phys. Rev. **D98**, 023014 (2018), `1803.08662`

[12] C. Meurer, J. Bluemer, R. Engel, A. Haungs, M. Roth, Czechoslovak Journal of Physics **56**, A211 (2006), `astro-ph/0512536`

[13] I. C. Maris (for the NA61/SHINE Collaboration), Proc. of 31st ICRC (2009)

[14] T. Pierog, K. Werner, Physical Review Letters **101**, 171101 (2008), `astro-ph/0611311`

[15] H.J. Drescher, Physical Review **D77**, 056003 (2008), `0712.1517`

[16] N. Abgrall et al. (NA61/SHINE Collaboration), Journal of Instrumentation **9**, P06005 (2014), `arXiv:1401.4699`

[17] N. Abgrall et al. (NA61/SHINE Collaboration), European Physics Journal **C76**, 84 (2016), `1510.02703`

[18] A. Aduszkiewicz et al. (NA61/SHINE Collaboration), European Physics Journal **C77**, 671 (2017), `1705.02467`

[19] K. Abe et al. (T2K Collaboration), Nuclear Instruments and Methods in Physics. **A659**, 106 (2011), `1106.1238`

[20] R. R. Prado (for the NA61/SHINE Collaboration), Proc. of 35th ICRC (2017), `1707.07902`

[21] E.J. Ahn, R. Engel, T.K. Gaisser, P. Lipari, T. Stanev, Physical Review **D80**, 094003 (2009), `0906.4113`

[22] R. Engel, F. Riehn, A. Fedynitch, T.K. Gaisser, T. Stanev, Proc. of 35th ICRC (2017)

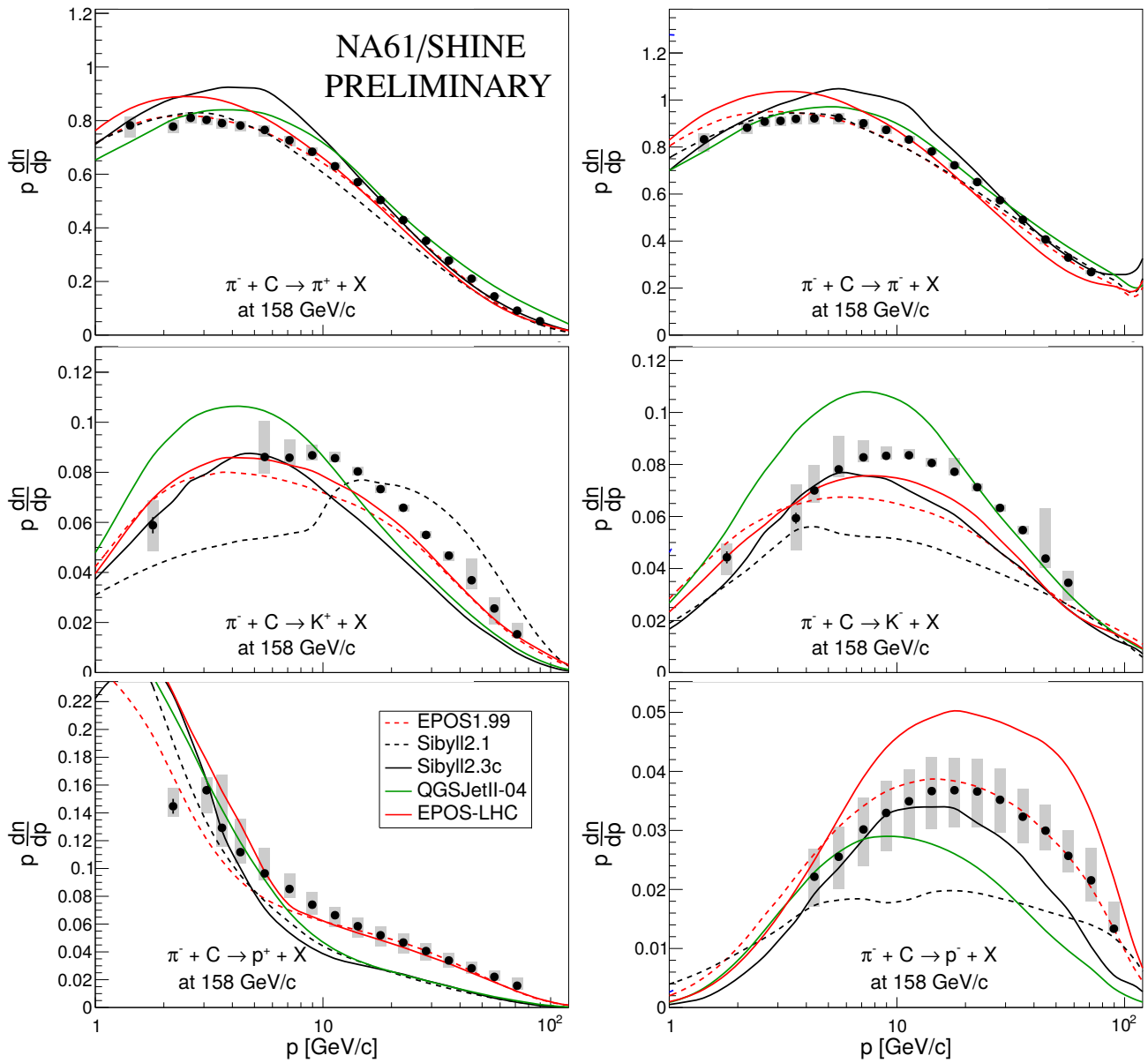[23] S. Ostapchenko, Physical Review **D83**, 014018 (2011), `1010.1869`

Figure 5: Spectra of $\pi^{\pm}$, $K^{\pm}$ and p($\bar{\text{p}}$) as a function of p (integrated over p_T), for the 158 GeV/c data set. The statistical uncertainties are shown as black bars and the systematic ones as gray bands.

[24] T. Pierog, I. Karpenko, J.M. Katzy, E. Yatsenko, K. Werner, Physical Review **C92**, 034906 (2015), `1306.0121`

[25] A. Herve (for the NA61/SHINE Collaboration), Proc. of 34th ICRC (2015), `1509.06586`

[26] R. R. Prado (for the NA61/SHINE Collaboration), in *7th International Conference on High Energy Physics in the LHC Era* (Valparaiso, Chile, 2018)

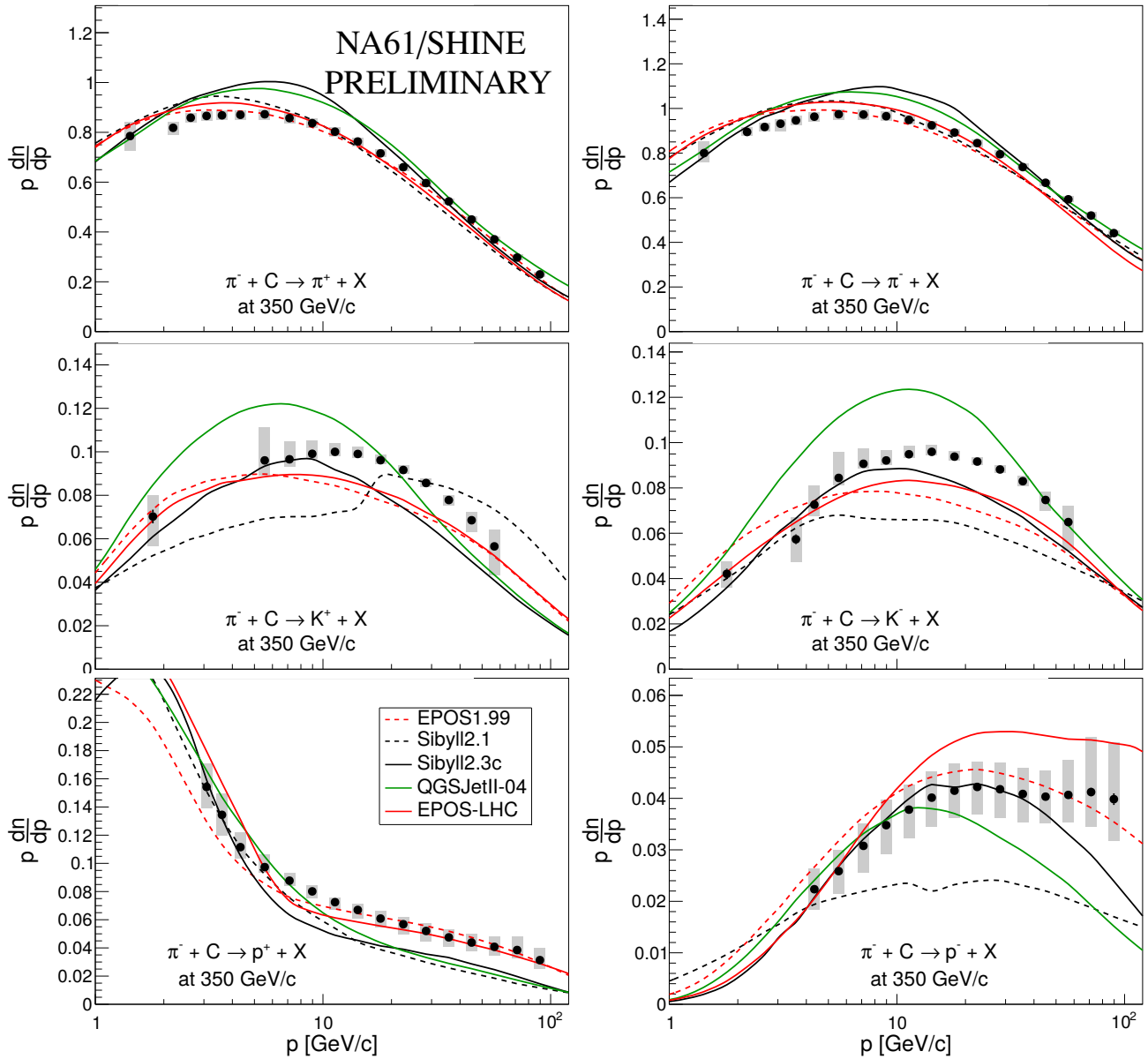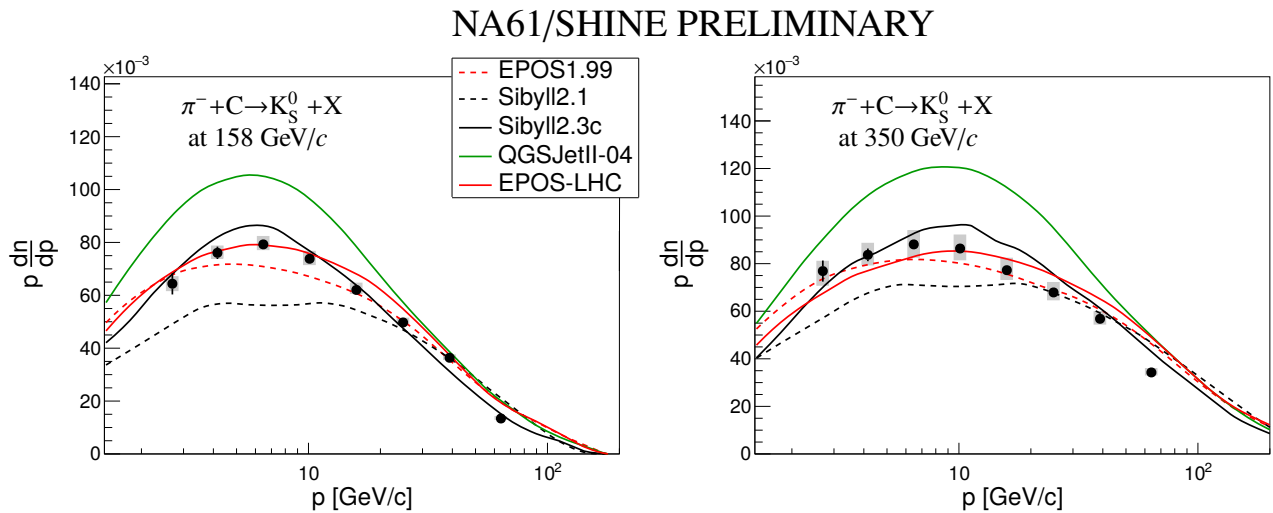[27] A. Aduszkiewicz et al. (NA61/SHINE Collaboration), European Physics Journal **C77**, 626 (2017), `1705.08206`

Figure 6: Spectra of $\pi^{\pm}$, $K^{\pm}$ and p($\bar{p}$) as a function of p (integrated over p_{T}), for the 350 GeV/c data set. The statistical uncertainties are shown as black bars and the systematic ones as gray bands.

Figure 7: Spectra of K^0_S as a function of p (integrated over p_{T}), for the 158 and 350 GeV/c data set. The statistical uncertainties are shown as black bars and the systematic ones as gray bands.
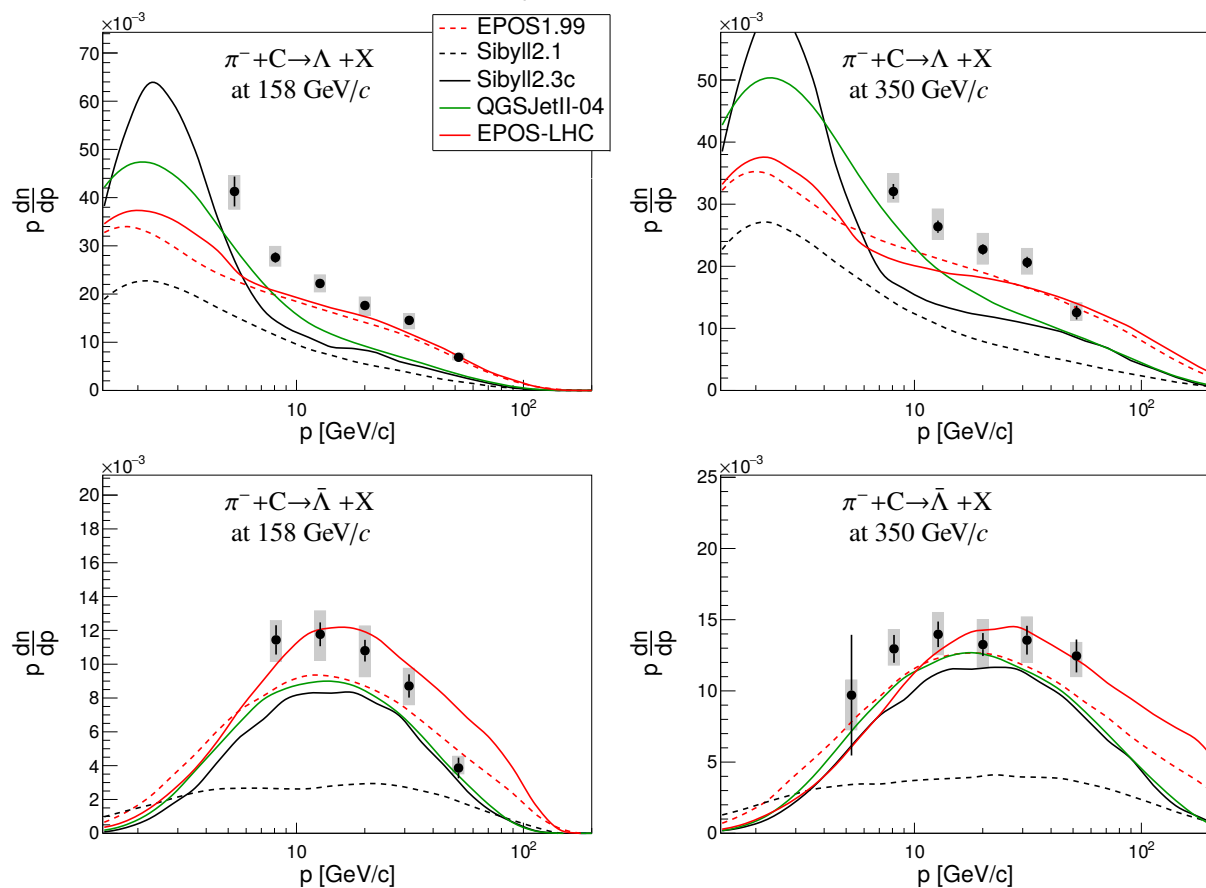
Figure 8: Spectra of $\Lambda(\bar{\Lambda})$ as a function of p (integrated over p_{T}), for the 158 and 350 GeV/c data set. The statistical uncertainties are shown as black bars and the systematic ones as gray bands.

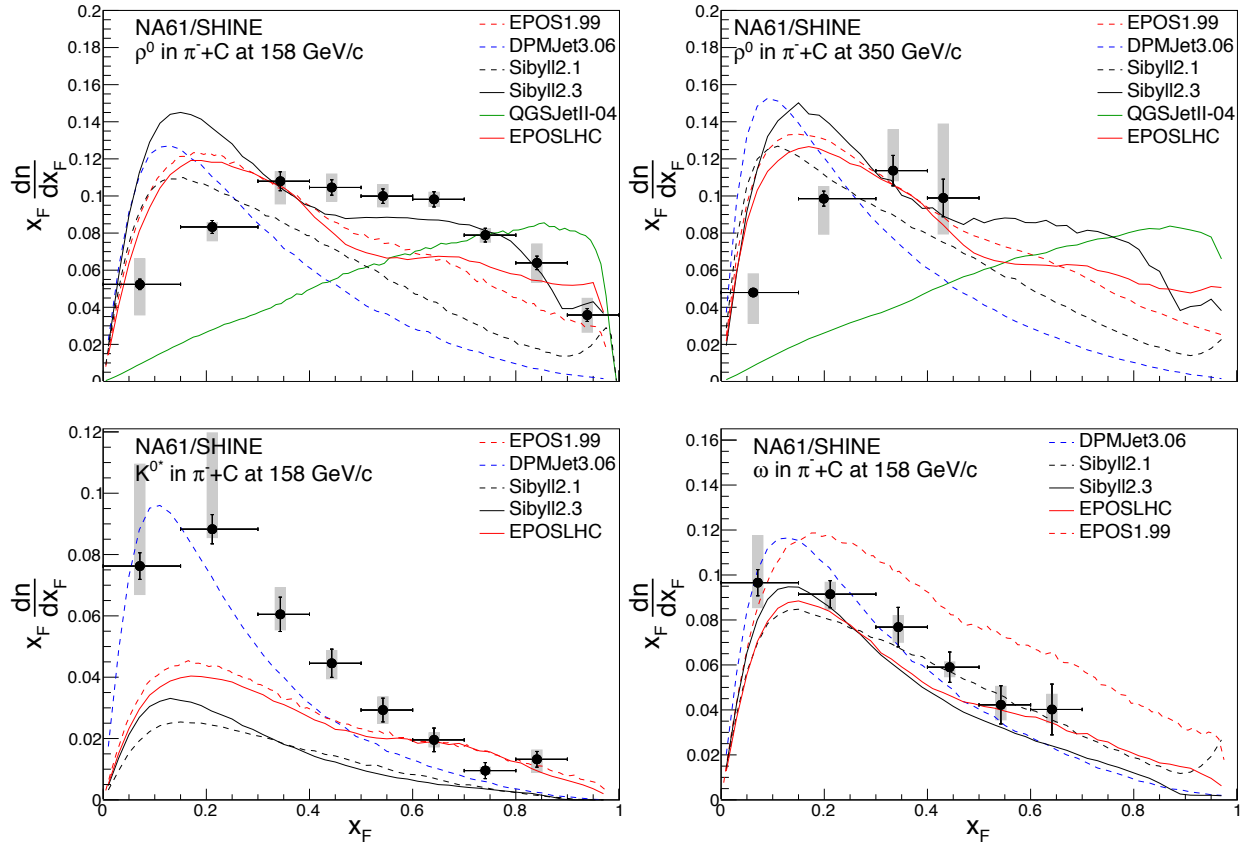**Figure 9**: Spectra of ρ^0, K^{*0} and ω as a function of x_F. The statistical uncertainties are shown as black bars and the systematic ones as gray bands.